DRAFT VERSION NOVEMBER 23, 2016
Preprint typeset using LaTeX style AASTeX6 v. 1.0

arXiv:1611.07035v1 [astro-ph.GA] 21 Nov 2016

A PROBABILISTIC APPROACH TO FITTING PERIOD-LUMINOSITY RELATIONS AND VALIDATING *GAIA* PARALLAXES

BRANIMIR SESAR[1], MORGAN FOUESNEAU[1], ADRIAN M. PRICE-WHELAN[2], CORYN A. L. BAILER-JONES[1], ANDY GOULD[1], AND HANS-WALTER RIX[1]

[1]Max Planck Institute for Astronomy, Königstuhl 17, D-69117 Heidelberg, Germany
[2]Department of Astrophysical Sciences, Princeton University, Princeton, NJ 08544, USA

ABSTRACT

Pulsating stars, such as Cepheids, Miras, and RR Lyrae stars, are important distance indicators and calibrators of the "cosmic distance ladder", and yet their period-luminosity-metallicity (PLZ) relations are still constrained using simple statistical methods that cannot take full advantage of available data. To enable optimal usage of data provided by the *Gaia* mission, we present a probabilistic approach that simultaneously constrains parameters of PLZ relations and uncertainties in *Gaia* parallax measurements. We demonstrate this approach by constraining PLZ relations of RR Lyrae stars in near-infrared W1 and W2 bands, using Tycho-Gaia Astrometric Solution (TGAS) parallax measurements for a sample of 123 RR Lyrae stars located within 2.5 kpc of the Sun. The fitted PLZ relations are consistent with previous studies, and in combination with other data, deliver distances precise to 6% (once various sources of uncertainty are taken into account). To a precision of 0.03 mas (1σ), we do not find a statistically significant offset in TGAS parallaxes for this sample of distant RR Lyrae stars (median parallax of 0.8 mas and distance of 1.4 kpc). With only minor modifications, our probabilistic approach can be used to constrain PLZ relations of other pulsating stars, and we intend to apply it to Cepheid and Mira stars in the near future.

Keywords: methods: data analysis — methods: statistical — parallaxes — stars: variables: RR Lyrae

1. INTRODUCTION

One of the main goals of observational astronomy is to ever more precisely and accurately measure the distance to astrophysical objects. Measuring distances to individual stars is critical to understanding a wide range of astronomical phenomena, from stellar structure to Galactic dynamics. An important tool in this endeavor are periodically-pulsating stars, such as Cepheids, Miras, and RR Lyrae stars, whose absolute magnitudes can be predicted using a period-luminosity (PL) relation[1], and whose period-luminosity relations can be calibrated using trigonometric parallax measurements (e.g., Feast & Catchpole 1997; van Leeuwen et al. 1997; Benedict et al. 2007, 2011). These stars and their PL relations are crucial, as they tie the extragalactic distance scale to the local one, and make the important second rung in the "cosmic distance ladder".

The trigonometric parallaxes (ϖ) obtained by the Tycho-Gaia Astrometric Solution (TGAS; Michalik et al. 2015), and made public through the Gaia Data Release 1 (Gaia Collaboration et al. 2016; Lindegren et al. 2016), present us with an exciting opportunity to recalibrate PL relations and potentially improve the accuracy of the cosmic distance ladder. However, the majority of Cepheids, Miras, and RR Lyrae stars in the TGAS sample are distant, and consequently, their parallaxes have a high fractional uncertainty ($\sigma_\varpi/\varpi > 0.2$). When a parallax has a high fractional uncertainty, the posterior probability distribution over its true distance is complex and non-Gaussian, even when the uncertainties in parallax are Gaussian (Bailer-Jones 2015; Astraatmadja & Bailer-Jones 2016). This poses a serious problem for the traditional approach to PL relation fitting, which assumes Gaussian uncertainties in distance, and does a weighted least-squares fit in the distance (i.e., absolute magnitude) vs. period plane. We can always, of course, fit PL relations by using only stars with precise parallaxes (and thus precise distances with close to Gaussian errors), but then we would ignore a large amount of potentially useful data (that was also obtained at a significant cost).

To avoid ignoring valuable data, in this paper we present a probabilistic approach to inferring period-luminosity(-metallicity) relations that makes a full use of parallax and other measurements, irrespective of their precision. To demonstrate the approach in practice, we use it to constrain period-luminosity-metallicity (PLZ) relations for RR Lyrae stars in the near-infrared W1 and W2 bands used by the WISE mission (Wright et al. 2010). While the demonstration is done using RR Lyrae stars, we emphasize that the approach can be easily applied to other pulsating stars, by simply plugging different data and prior information into our framework.

In addition to constraining PLZ relations, our approach enables a straightforward validation of parallax measurements

bsesar@mpia.de

[1] The period-luminosity relation for Cepheids is also known as the Leavitt law (Leavitt 1908; Leavitt & Pickering 1912).

and their uncertainties. The validation of parallaxes is important as several studies have reported an offset in TGAS parallaxes (Stassun & Torres 2016; Jao et al. 2016) and an overestimation of TGAS parallax uncertainties (Casertano et al. 2016; Gould et al. 2016).

Our paper is organized as follows. In Section 2, we describe the astrometric, photometric, and spectroscopic data used to calibrate PLZ relations for RR Lyrae stars in WISE W1 and W2 bands, and validate TGAS parallaxes. The construction of the likelihood function that is at the core of our probabilistic approach, is presented in Section 3. In Section 4, we present the results of applying the probabilistic method of Section 3, to data described in Section 2. We summarize and discuss our results in Section 5.

2. DATA

To constrain the PLZ relations for RR Lyrae stars in WISE W1 and W2 bands, we use TGAS trigonometric parallaxes (ϖ), spectroscopic metallicities ([Fe/H]; Fernley et al. 1998), log-periods ($\log P$, base 10), and apparent magnitudes[2] (m; Klein et al. 2014) for 123 RR Lyrae stars within $\approx$ 2.5 kpc from the Sun. The $E(B-V)$ reddening at a star's position is obtained from the Schlegel et al. (1998) dust map. We denote this data set as $\mathcal{D} = \{\mathbf{d_k}\}$, where $\mathbf{d_k} = \{\varpi, [\mathrm{Fe/H}], \log P, m, EBV\}$ is the data set associated with the kth star.

Briefly, the stars in our sample have metallicities ranging from -0.1 dex to -2.6 dex, and periods ranging from 0.36 to 0.73 days. The uncertainty in [Fe/H] is the same for all stars, $\sigma_{[\mathrm{Fe/H}]} = 0.15$ dex (see Note 8 in Table 1 of Fernley et al. 1998). Based on the analysis of Klein et al. (2011, see their Appendix A), we assume that the uncertainty in log-period is $\sigma_{\log \mathrm{P}} = 0.02 \log P$. The uncertainty in $E(B-V)$ is assumed to be $\sigma_{\mathrm{EBV}} = 0.1E(B-V)$ (Schlegel et al. 1998). The average uncertainty in apparent magnitudes is $\sigma_{\mathrm{m}} = 0.005$ mag (Klein et al. 2014).

The TGAS parallax measurements have reported uncertainties ranging from 0.22 mas to 0.47 mas (5th to 95th percentile), with a median of 0.28 mas. The median fractional uncertainty of our sample is $\sigma_\varpi/\varpi = 0.17$. As described by Lindegren et al. (2016), the reported parallax uncertainties were calculated as (their Equation 4)

$$\sigma_\varpi = \sqrt{(f_\varpi \varsigma_\varpi)^2 + \sigma^2_{\varpi,\mathrm{add}}}, \tag{1}$$

where ς_ϖ is the formal parallax uncertainty, $f_\varpi = 1.4$, and $\sigma_{\varpi,\mathrm{add}} = 0.2$ mas. To facilitate validation of TGAS parallax uncertainties in Section 3, we calculate ς_ϖ values as

$$\varsigma_\varpi = \sqrt{\sigma^2_\varpi - (0.20/1000)^2}/1.4 \tag{2}$$

3. METHOD

Using the above data set $\mathcal{D}$, we now wish to constrain parameters a, b, M_{ref}, and σ_{M} that define the (noisy) PLZ relation

$$M = a\log(P/P_{\mathrm{ref}}) + b([\mathrm{Fe/H}] - [\mathrm{Fe/H}]_{\mathrm{ref}}) + M_{\mathrm{ref}} + \epsilon, \tag{3}$$

where P is the period of pulsation, M_{ref} is the absolute magnitude at some reference period P_{ref} and metallicity $[\mathrm{Fe/H}]_{\mathrm{ref}}$ (here set to the median period and metallicity of the sample described in Section 2, $P_{\mathrm{ref}} = 0.52854$ days and $[\mathrm{Fe/H}]_{\mathrm{ref}} = -1.4$ dex), and a and b scale the absolute magnitude with log-period and metallicity, respectively.

The ϵ is a standard normal random variable with zero mean and standard deviation σ_{M} that, in principle, accounts for the scatter in absolute magnitude M due to modeling uncertainties. When interpreting this scatter, however, it is important to keep in mind that in reality, σ_{M} is *convolved* with unaccounted measurement uncertainties. Thus, σ_{M} represents the so-called "intrinsic" scatter in a PLZ relation only if the measurement uncertainties are correctly estimated (which is difficult to do in practice).

As mentioned above, we also allow freedom in the error model used for the parallax measurements. We model the TGAS parallax measurements as being drawn from a Gaussian distribution centered on

$$\varpi' = 1/r + \varpi_0, \tag{4}$$

where r is the true heliocentric distance (in parsecs), and ϖ_0 represents the global offset of TGAS parallaxes with respect to the inverse distances (e.g., an offset due to the impact of imperfectly modeled basic-angle variations on the astrometric solution; Lindegren et al. 2016). The standard deviation of this Gaussian is equal to the uncertainty in the TGAS parallax, which we model using Equation 1, where f_ϖ and $\sigma_{\varpi,\mathrm{add}}$ are also included as free parameters. The expressions defined by Equations 4 and 1 were motivated by conclusions of recent studies that have found TGAS parallaxes to be offset (Jao et al. 2016; Stassun & Torres 2016; De Ridder et al. 2016), and studies that have found TGAS parallax uncertainties to be overestimated (Gould et al. 2016; Casertano et al. 2016).[3]

To constrain the PLZ relation in a probabilistic manner we need to calculate the joint posterior probability $p(\boldsymbol{\theta}_{\mathrm{PLZ}}, \boldsymbol{\theta}_\varpi, \{\boldsymbol{\alpha}_k\} \,|\, \mathcal{D})$, given the data set $\mathcal{D}$, of the PLZ parameter value set $\boldsymbol{\theta}_{\mathrm{PLZ}} = \{a, b, M_{\mathrm{ref}}, \sigma_{\mathrm{M}}\}$, the TGAS parallax validation parameters $\boldsymbol{\theta}_\varpi = \{\varpi_0, f_\varpi, \sigma_{\varpi,\mathrm{add}}\}$, and the set of nuisance parameters $\boldsymbol{\alpha}_k = \{r, \log P^{\mathrm{int}}, [\mathrm{Fe/H}]^{\mathrm{int}}, EBV^{\mathrm{int}}, M^{\mathrm{int}}\}_k$ that represent the true distance r, intrinsic log-period $\log P^{\mathrm{int}}$, metallicity $[\mathrm{Fe/H}]^{\mathrm{int}}$, reddening EBV^{int}, and absolute magnitude M^{int} for each star. For conciseness, we also define $\boldsymbol{\theta} = (\boldsymbol{\theta}_{\mathrm{PLZ}}, \boldsymbol{\theta}_\varpi)$. For this work, our main interest is in the marginal posterior probability of the PLZ and TGAS validation parameters $p(\boldsymbol{\theta} \,|\, \mathcal{D})$, which is related to the marginal likelihood $p(\mathcal{D} \,|\, \boldsymbol{\theta})$ through

$$p(\boldsymbol{\theta} \,|\, \mathcal{D}) \propto p(\mathcal{D} \,|\, \boldsymbol{\theta})\, p(\theta), \tag{5}$$

where $p(\boldsymbol{\theta})$ is the prior probability of the parameter value set

[2] Averaged in flux over a pulsation period.

[3] Note that these models can be easily extended: For example, we could model the dependence of parallax on ecliptic latitude by simply adding a $b_\varpi \beta$ term to Equation 4, where b_ϖ is a new model parameter, and β is the ecliptic latitude of a star (in units of arcsec).

$\boldsymbol{\theta}$, and

$$p(\mathcal{D}\,|\,\boldsymbol{\theta}) = \prod_k p(\mathbf{d_k}\,|\,\boldsymbol{\theta}) \tag{6}$$

$$= \prod_k \int p(\mathbf{d_k}\,|\,\boldsymbol{\theta}, \boldsymbol{\alpha}_k)\, p(\boldsymbol{\alpha}_k)\, \mathrm{d}\boldsymbol{\alpha}_k \tag{7}$$

is the marginal likelihood of the full data set given the combined PLZ parameter values and TGAS validation parameters ($\boldsymbol{\theta}$), and assuming independent data points.

The (un-marginalized) likelihood function for the kth star is given as follows:

$$\begin{aligned} p(\mathbf{d_k}\,|\,\boldsymbol{\theta}, \boldsymbol{\alpha}_k) &= p(M\,|\,M^{\rm int}, \boldsymbol{\theta}_{\rm PLZ}) \\ &\times p(\log P\,|\,\log P^{\rm int})\, p([{\rm Fe/H}]\,|\,[{\rm Fe/H}]^{\rm int}) \\ &\times p(EBV\,|\,EBV^{\rm int})\, p(\varpi\,|\,r, \boldsymbol{\theta}_\varpi) \\ &\times p(m\,|\,r, M^{\rm int}, EBV^{\rm int}, A_\lambda), \end{aligned} \tag{8}$$

where:

$$\mathcal{N}(x\,|\,\mu, \sigma^2) = \frac{1}{\sqrt{2\pi\sigma^2}} \exp\left(-\frac{1}{2}\frac{(x-\mu)^2}{\sigma^2}\right) \tag{9}$$

is a normal distribution centered on μ with variance σ^2, and

$$p(M\,|\,M^{\rm int}, \boldsymbol{\theta}_{\rm PLZ}) = \mathcal{N}(M\,|\,M^{\rm int}, \sigma^2_{\rm M}) \tag{10}$$

$$M = a\,\log(P^{\rm int}/P_{\rm ref}) + b\,([{\rm Fe/H}]^{\rm int} - [{\rm Fe/H}]_{\rm ref}) + M_{\rm ref} \tag{11}$$

$$p(\log P\,|\,\log P^{\rm int}) = \mathcal{N}(\log P\,|\,\log P^{\rm int}, \sigma^2_{\log {\rm P}}) \tag{12}$$

$$p([{\rm Fe/H}]\,|\,[{\rm Fe/H}]^{\rm int}) = \mathcal{N}([{\rm Fe/H}]\,|\,[{\rm Fe/H}]^{\rm int}, \sigma^2_{[{\rm Fe/H}]}) \tag{13}$$

$$p(EBV\,|\,EBV^{\rm int}) = \mathcal{N}(EBV\,|\,EBV^{\rm int}, \sigma^2_{\rm EBV}) \tag{14}$$

$$p(\varpi\,|\,r, \boldsymbol{\theta}_\varpi) = \mathcal{N}(\varpi\,|\,\varpi', \sigma^2_\varpi) \tag{15}$$

$$p(m\,|\,r, M^{\rm int}, EBV^{\rm int}, A_\lambda) = \mathcal{N}(m\,|\,m', \sigma^2_m) \tag{16}$$

$$m' = M^{\rm int} + A_\lambda EBV^{\rm int} + 5\log r - 5 \tag{17}$$

Our statistical model is also visualized as a probabilistic graphical model (PGM) shown in Figure 1. One of the advantages of PGMs is that they enable a straightforward examination of dependencies between data and model parameters (Koller & Friedman 2009). For example, while the observed apparent magnitude m depends on the intrinsic absolute magnitude $M^{\rm int}$ and heliocentric distance r, the observed parallax ϖ depends only on distance (and TGAS parallax validation parameters, θ_ϖ, described above).

In the above equations, we model the observed log-period, metallicity, reddening, as well as the absolute magnitude predicted by the PLZ relation (M), as being drawn from Gaussian distributions centered on some "intrinsic" values (represented by the superscript "int"), and with a standard deviation equal to the uncertainty in measurement or the model. The "int" parameters are "intrinsic" in the sense that they are not affected by uncertainties (model or observational).

Note that Equation 8 contains 7 global parameters (4 in $\boldsymbol{\theta}_{\rm PLZ}$ and 3 in $\boldsymbol{\theta}_\varpi$ parameter sets), and 5 *nuisance* parameters for each star, $\boldsymbol{\alpha}_k$. Since we are (at the moment) not interested

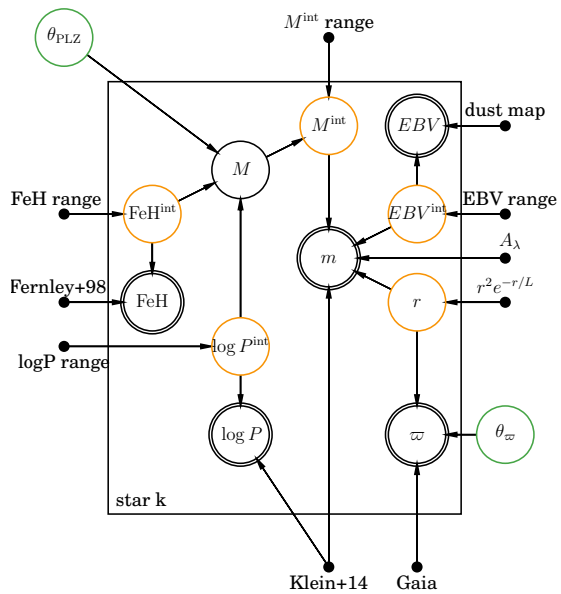

Figure 1. The probabilistic graphical model that describes the dependencies between model parameters and data used in this work. Double circles indicate likelihoods, single orange circles indicate nuisance parameters, while single green circles indicate model parameter sets. Fixed parameters, such as the extinction coefficient (A_λ; Schlafly et al. 2016), priors on nuisance parameters (e.g., $M^{\rm int}$ range), as well as data sources (e.g., Gaia), are not enclosed in circles. "M" is a just a placeholder for the PLZ relation (Equation 11). Parameters inside the square are specific to the kth star, while those on the outside are global. The arrows indicate conditional dependence. For example, the arrows from r and θ_ϖ to ϖ indicate that the observed parallax ϖ depends on the heliocentric distance r and TGAS parallax validation parameters θ_ϖ (i.e., $p(\varpi\,|\,r, \boldsymbol{\theta}_\varpi)$).

in these nuisance parameters, we marginalize (i.e. integrate) Equation 8 over these parameters.

We use the following prior probability distributions for the nuisance parameters $\boldsymbol{\theta}_\varpi$. For $[{\rm Fe/H}]^{\rm int}$, $\log P^{\rm int}$, and $M^{\rm int}$, we choose priors that are uniform in ranges appropriate for RR Lyrae stars: 0 dex to -3 dex, -1.0 $\log({\rm day})$ to 0 $\log({\rm day})$, and -2 mag to 0.2 mag (based on the range of absolute K-band magnitudes listed in Table 3 of Marconi et al. 2015). For $EBV^{\rm int}$, we adopt a uniform prior in the 0 mag to 1 mag range (appropriate for low-extinction regions, as is the case here), and for distance, we adopt an exponentially decreasing volume density prior with a scale length $L = 500$ pc (Bailer-Jones 2015; Astraatmadja & Bailer-Jones 2016)

$$p(r) = 1/(2L^3)\, r^2\, \exp(-r/L), \tag{18}$$

which we define to be positive in the $200 < r/{\rm pc} < 2700$ distance range, and zero elsewhere. We chose $L = 500$ pc as this value minimizes the scatter in the PLZ relation, $\sigma_{\rm M}$, for our sample of RR Lyrae stars.

The marginal likelihood for the kth star is

$$p(\mathbf{d_k}\,|\,\boldsymbol{\theta}) = \int \mathrm{d}\boldsymbol{\alpha}_k\, p(\mathbf{d_k}\,|\,\boldsymbol{\theta}, \boldsymbol{\alpha}_k)\, p(\boldsymbol{\alpha}_k) \tag{19}$$

which can be written in a simpler form by analytically performing the integrals over the Gaussian expressions in

$\log P^{\rm int}$, $[{\rm Fe/H}]^{\rm int}$, $EBV^{\rm int}$, and $M^{\rm int}$:

$$p(\mathbf{d_k}\,|\,\boldsymbol{\theta}) \propto \int_{200\,pc}^{2700\,pc} {\rm d}r\, \mathcal{N}(\varpi\,|\,\varpi', \sigma_\varpi^2) \times \mathcal{N}(DM'\,|\,DM, \sigma_{\rm DM}^2)\, p(r), \qquad (20)$$

where

$$DM = 5\log r - 5$$
$$DM' = m - A_\lambda EBV - (a\log(P/P_{\rm ref}) + b([{\rm Fe/H}] - [{\rm Fe/H}]_{\rm ref}) + M_{\rm ref})$$
$$\sigma_{\rm DM}^2 = \sigma_m^2 + (a\sigma_{\rm logP})^2 + (b\sigma_{[{\rm Fe/H}]})^2 + (A_\lambda \sigma_{\rm EBV}^2) + \sigma_M^2$$

The likelihood for the entire data set $\mathcal{D}$ can now be calculated using Equation 6.

Before we can calculate the (marginal) posterior distribution (Equation 5), we need to define prior probabilities for the global parameters $\boldsymbol{\theta}_{\rm PLZ}$ and $\boldsymbol{\theta}_\varpi$. For $\sigma_{\rm M}$ and $\sigma_{\varpi,{\rm add}}$ we adopt Jeffreys log-uniform priors ($p(x) \propto 1/x$; Jaynes 1968), and for the b parameter that scales the absolute magnitude with $\log P$, we require that $b > 0$ (based on stellar evolution and pulsation models of RR Lyrae stars; Marconi et al. 2015). Since the ϖ' parameter must be positive (Equation 4), we require that $\varpi_0 > -1/r$ at $r = 200$ pc (i.e., $\varpi_0 > -5$ mas). For the remaining model parameters we adopt wide uniform priors.

To efficiently explore the parameter space, we use the Goodman & Weare (2010) Affine Invariant Markov chain Monte Carlo (MCMC) Ensemble sampler as implemented in the `emcee` package[4] (v2.2.1, Foreman-Mackey et al. 2013). We use 160 walkers and obtain convergence[5] after a burn-in phase of 1000 steps per walker. The chains are then restarted and evolved for another 500 steps.

To describe the marginal posterior distributions of individual model parameters, we measure the median, the difference between the 84th percentile and the median, and the difference between the median and the 16th percentile of each marginal posterior distribution (for a Gaussian distribution, these differences are equal to ± 1 standard deviation). We report these and maximum a posteriori (MAP) values in Table 1.

Table 1. PLZ Relations and TGAS Parallax Validation Parameters

Band	a (mag dex^{-1})	b (mag dex^{-1})	$M_{\rm ref}$ (mag)	$\sigma_{\rm M}$ (mag)	ϖ_0 (mas)	f_ϖ	$\sigma_{\varpi,{\rm add}}$ (mas)
W1	$-1.54^{+0.69}_{-0.64}$	$0.25^{+0.09}_{-0.08}$	$-0.62^{+0.08}_{-0.07}$	$0.06^{+0.06}_{-0.03}$	$0.02^{+0.04}_{-0.04}$	$0.98^{+0.29}_{-0.31}$	$0.16^{+0.04}_{-0.04}$
	-1.50	0.27	-0.61	0.05	0.01	1.0	0.16
W2	$-1.48^{+0.65}_{-0.63}$	$0.26^{+0.08}_{-0.08}$	$-0.65^{+0.07}_{-0.07}$	$0.05^{+0.05}_{-0.03}$	$0.03^{+0.03}_{-0.03}$	$0.90^{+0.33}_{-0.36}$	$0.18^{+0.04}_{-0.04}$
	-1.48	0.30	-0.66	0.04	0.04	0.98	0.17

NOTE—In each band, the first line lists the median, the difference between the 84th percentile and the median, and the difference between the median and the 16th percentile of each marginal posterior distribution. The second line provides the maximum a posteriori (MAP) values.

4. RESULTS

In this Section, we discuss PLZ relations and TGAS parallax validation parameters that we have constrained by applying the method described in Section 3, to data described in Section 2. To illustrate the correlations between various model parameters, in Figure 2 we show two-dimensional posterior distributions for parameter pairs. The parameters we constrain also allow us to calculate more precise distances to RR Lyrae stars in our sample (Table 2).

4.1. *PLZ Parameters*

We find that, within the uncertainties, the PLZ parameters obtained using W1 band data are consistent with those obtained using W2 band data. This result is not too surprising given i) fairly large uncertainties in parameters, ii) the proximity of W1 and W2 bands in wavelength, and iii) the fact that the parameters of PL(Z) relations change little with wavelength for bands redder than the H or K band (Catelan et al. 2004; Marconi et al. 2015; Figure 4 of Madore et al. 2013). Since the two PLZ relations are consistent, we use PLZ parameters for the W2 band when comparing relations to previous studies.

Even though we find the period slope of the PLZ relation (i.e., parameter a) to be flatter compared to the one found by previous observational studies (-1.5 vs. -2.3, Madore et al. 2013; Klein et al. 2014; Dambis et al. 2014), the two values are still consistent within $\approx 1\sigma$ of uncertainties. The metallicity slope of the PLZ relation (i.e., parameter b) is steeper than the value found by Dambis et al. (2014, 0.26 vs. 0.1), making the two values (in)consistent at the 1.7σ level.

When comparing values of parameters with the results obtained by previous studies, it is also important to consider correlations between parameters. As Figure 2 shows, the slopes in period and metallicity are correlated (i.e., parameters a and b); as the value of parameter a decreases, so does

[4] http://dan.iel.fm/emcee/current/

[5] We checked for convergence of chains by examining the autocorrelation time of the chains per dimension.

the value of parameter b. For example, if we assume that the true value of parameter a is in the vicinity of the value found by Dambis et al. (2014), $a = -2.27 \pm 0.13$ mag dex^{-1}, we can impose a Gaussian prior $\mathcal{N}(a|-2.27, 0.12)$ on the period slope a when calculating the posterior distribution (instead of a uniform prior, as done in Section 3). In that case, the resulting $b = 0.21 \pm 0.07$ mag dex^{-1} agrees more closely with the metallicity slope of 0.12 ± 0.02 found by Dambis et al. (2014).

The reference absolute magnitude we have measured for the W2 band, $M_{\rm ref} = -0.65 \pm 0.07$ mag, is more precise than the $M_{\rm ref} = -0.62 \pm 0.09$ mag predicted by the PLZ relation of Dambis et al. (2014), most likely due to a much larger number of stars with parallax measurements in our sample (123 stars with TGAS parallaxes vs. 5 stars with HST parallaxes).

The $\sigma_{\rm M}$ MAP values[6] of 0.05 mag and 0.04 mag for W1 and W2 bands, respectively, seem a bit high given the expectation of a small intrinsic scatter in near-IR PLZ relations (Table 6 of Marconi et al. 2015). However, recall that $\sigma_{\rm M}$ is *convolved* (via Equation 3) with unaccounted measurement uncertainties in apparent magnitude, metallicity, and log-period. One possible source of unaccounted uncertainties may be the scatter in the WISE magnitude zeropoint, which is ≈ 0.03 mag (Table 8 of Section 4.4.h Explanatory Supplement to the WISE All-Sky Data Release Products[7]). Another source may be the uncertainty in [Fe/H], which Fernley et al. (1998) estimated at 0.15 dex, but that could be higher since the [Fe/H] values reported by Fernley et al. (1998) are actually a compilation of metallicities measured by different studies.

4.2. *TGAS Parallax Validation Parameters*

We measure the ϖ_0 parameter (that models the global offset of TGAS parallax measurements) to be consistent with zero within 0.03 mas (i.e., $\varpi_0 = 0.03 \pm 0.03$ mas), indicating that there is no statistically significant offset in parallax, at least for this sample of distant RR Lyrae stars (median distance ≈ 1 kpc).

Five RR Lyrae stars in our sample (SU Dra, RR Lyr, UV Oct, XZ Cyg, and RZ Cep) also have parallaxes measured by Benedict et al. (2011) using Hubble Space Telescope (HST) astrometric observations. We find the average of the difference between TGAS and HST parallax measurements to be 0.04 mas, in agreement with our $\varpi_0 = 0.03 \pm 0.03$ mas measurement.

Regarding the renormalization of TGAS formal parallax uncertainties ς_ϖ (see Equation 1), we find $\sigma_{\varpi,\rm add} = 0.18$ mas and that f_ϖ is consistent with 1 within uncertainties (i.e., $f_\varpi = 0.9 \pm 0.3$). Since f_ϖ is consistent with 1, and since f_ϖ needs to be greater or equal than 1 (according to the Cramér-Rao bound; Cramér 1999), we assume that $f_\varpi = 1$.

[6] Since the marginal posterior distribution of $\sigma_{\rm M}$ is quite asymmetric (Figure 2), we discuss the MAP value as it is closer to the mode of the marginal distribution.

[7] http://wise2.ipac.caltech.edu/docs/release/allsky/expsup/sec4_4h.html

4.3. *Distances*

As we have mentioned in Section 1, measuring precise and accurate distances to stars is of great importance for many fields in astronomy. The same probabilistic approach we have used in Section 3 now allows us to constrain distances to stars in our sample by taking all the available data (and their uncertainties) into account. These data include individual measurements, such as TGAS parallaxes, as well as information derived from modeling RR Lyrae stars as a population, such as PLZ relations and the parameters that model uncertainties in TGAS parallaxes.

Using relations of conditional probability, the marginal posterior distribution of the heliocentric distance for the kth star can be written as

$$p(r_k \,|\, \mathbf{d_k}, \boldsymbol{\theta}) \propto p(r) \int \mathrm{d}\boldsymbol{\theta}\, \mathcal{N}(\varpi \,|\, \varpi', \sigma^2_\varpi) \times \mathcal{N}(DM' \,|\, DM, \sigma^2_{\rm DM}), \quad (21)$$

where Equation 21 is being integrated (i.e., marginalized) over parameters contained in $\boldsymbol{\theta}_{\rm PLZ}$ and $\boldsymbol{\theta}_\varpi$ sets[8].

We evaluate Equation 21 over the $200 < r/{\rm pc} < 2700$ distance range and average it over 160 samples of $\boldsymbol{\theta}_{\rm PLZ}$ and $\boldsymbol{\theta}_\varpi$ parameters taken from the last step of the Markov chain (which has 160 walkers). The $p(r_k \,|\, \mathbf{d_k}, \boldsymbol{\theta})$ is then characterized by fitting a Gaussian to it. We list the distances and their uncertainties in Table 2. The median of the fractional uncertainty in distance is 6%.

Table 2. Distances to RR Lyrae Stars

Name	Heliocentric distance (pc)
RRLyr	271.8 ± 10.4
FWLup	377.5 ± 19.4
CSEri	512.1 ± 30.0

NOTE—A machine readable version of this table is available in the electronic edition of the Journal. A portion is shown here for guidance regarding its form and content.

5. SUMMARY AND CONCLUSIONS

In this Letter, we have presented a probabilistic method that simultaneously constrains a period-luminosity-metallicity (PLZ) relation and validates (TGAS) parallax measurements. Compared to the traditionally-used weighted least-squares fitting of a PLZ relation, our approach allows for a direct usage of parallax (and other) measurements, while accounting fully for their precision. In comparison,

[8] The marginalization over $M^{\rm int}$, $\log P^{\rm int}$, $[{\rm Fe/H}]^{\rm int}$, and $EBV^{\rm int}$ parameters is implicit in the expression for $\mathcal{N}(DM' \,|\, DM, \sigma^2_{\rm DM})$ (see Equation 19).

the traditional approach cannot use imprecise parallaxes as their transformation into distance, and the subsequent characterization of the uncertainty in distance, is not a trivial task (Bailer-Jones 2015; Astraatmadja & Bailer-Jones 2016).

The final product of our approach is the full posterior distribution of all model parameters (in the form of a Markov chain). The posterior distribution enables a more general description of model parameters and their correlations (see Figure 2). For example, the marginal posterior distribution (i.e., the histogram) of $\sigma_{\rm M}$ in Figure 2 clearly shows that this parameter cannot be described by a Gaussian, which is something the traditional approach would be forced to do. Furthermore, the non-linear correlation between f_ϖ and $\sigma_{\varpi,\rm add}$ is beautifully described by the joint posterior distribution of these two parameters (see Figure 2). The least-squares approach would be hard-pressed to capture such complexities.

We have used this probabilistic approach to constrain the PLZ relations in the near-IR W1 and W2 bands used by the WISE mission. Overall, the PLZ parameters we recover are consistent (within uncertainties) with the parameters found by previous studies (Madore et al. 2013; Klein et al. 2014; Dambis et al. 2014). Due to the fairly high fractional parallax uncertainty of our sample (median $\sigma_\varpi/\varpi \approx 0.17$), we were not able to constrain the slopes in log-period and metallicity more precisely than Dambis et al. (2014). However, since Dambis et al. (2014) used iterative least-squares fitting to constrain PLZ relations and fairly *ad hoc* removal of outlying data points, it is possible that their uncertainties may be underestimated. The second release of Gaia data, scheduled for late 2017, will provide more accurate and precise parallax measurements, and based on our current experience, is expected to place significantly tighter constraints on PLZ relations of RR Lyrae and other pulsating stars.

Since obtaining precise and accurate measurements of $[{\rm Fe/H}]$ for RR Lyrae stars is not a trivial task (e.g., see Nemec et al. 2013), the optimal data set for constraining PLZ relations for RR Lyrae stars may need to contain field *and* globular cluster RR Lyrae stars. By being at the same distances and by having the same (and precisely measured) $[{\rm Fe/H}]$, globular cluster RR Lyrae stars could be used to constrain the period and metallicity dependence of the PLZ relation (i.e., parameters a and b), while a few field RR Lyrae stars with well-measured Gaia parallaxes and $[{\rm Fe/H}]$ (e.g., those observed by Nemec et al. 2013) would constrain the zero-point of the PLZ relation. Such datasets were used by Sollima et al. (2006) and Dambis et al. (2014), but these studies used least-squares fitting to constrain PLZ relations. In the future, we may apply our method to the same datasets.

While constraining PLZ relations, we also simultaneously constrained parameters that model TGAS parallax measurements and their uncertainties. To a precision of 0.03 mas, we did not find a statistically significant offset in TGAS parallaxes (i.e., the global offset parameter $\varpi_0 = 0.03 \pm 0.03$ mas) using our sample of distant RR Lyrae stars (median parallax of 0.8 mas and distance of 1.4 kpc). This result is consistent with the conclusion of Casertano et al. (2016), who use photometric parallaxes of distant Cepheids (median distance of ≈ 2 kpc) and find no offset to a precision of 0.02 mas.

The fact that we do not detect an offset in TGAS parallaxes may even be consistent with the findings of Stassun & Torres (2016) and Jao et al. (2016), who measure a global offset of ≈ -0.25 mas in TGAS parallaxes, but suggest that it may become negligible for parallaxes smaller than a few mas (i.e., at large distances). However, given the manner in which the trigonometric parallax measurements are made (linear offsets on the detector), we do not understand what physical effect could cause a distance-dependent offset in TGAS parallaxes.

Regarding the uncertainty in TGAS parallaxes, we find no need to rescale formal parallax uncertainties *for RR Lyrae stars* (i.e., no need for $f_\varpi > 1$), and recommend the following equation when calculating their uncertainty in parallax

$$\sigma_{\varpi,\rm RRLyr} = \sqrt{(1.0\varsigma_\varpi)^2 + (0.18/1000)^2}, \qquad (22)$$

where the formal parallax uncertainty ς_ϖ can be calculated using Equation 2. The $f_\varpi = 1.1$ and $\sigma_{\varpi,\rm add} = 0.12$ mas values obtained by Gould et al. (2016) are consistent at the 1σ level with our findings.

We emphasize that our and Gould et al. (2016) results for f_ϖ and $\sigma_{\varpi,\rm add}$ were obtained using RR Lyrae stars. Due to as yet uncalibrated systematic effects in *Gaia* measurements, stars with different properties (e.g., color, brightness) may have different f_ϖ and $\sigma_{\varpi,\rm add}$ values. Various systematic effects may also explain the values of $f_\varpi = 1.4$ and $\sigma_{\varpi,\rm add} = 0.20$ mas that Lindegren et al. (2016) adopted for TGAS. Unlike us, Lindegren et al. (2016) used a much more diverse sample of stars when constraining these two parameters (see their Appendix C.1).

By using individual measurements (e.g., TGAS parallaxes), PLZ relations, and parameters that model uncertainties in TGAS parallaxes, we have constrained distances to ≈ 120 RR Lyrae stars within 2.5 kpc of the Sun, to a 6% precision. While this precision may seem quite low compared to precisions reported in some previous studies (e.g., a 0.8% precision reported by Klein et al. 2014), we note that our estimate includes uncertainties due to correlations (e.g., between the period and metallicity slopes in the PLZ relation), and accounts for underestimated or unaccounted uncertainties in measurements and the model (via the $\sigma_{\rm M}$ parameter). Studies that did not take such uncertainties into account, and did not propagate them properly through the model, have likley overestimated the precision of their distance measurements.

In conclusion, we are looking forward to applying the method and the experience developed in this work to the next Gaia data release, and doing some exciting Galactic science with Cepheid, Mira, and RR Lyrae stars in the near future.

B.S. and H.-W.R. acknowledge funding from the European Research Council under the European Unions Seventh Framework Programme (FP 7) ERC Grant Agreement n. [321035]. This project was developed in part at the 2016 NYC Gaia Sprint, hosted by the Center for Computational Astrophysics at the Simons Foundation in New York City. This work has made use of data from the European Space Agency (ESA) mission Gaia (http://www.cosmos.esa.int/gaia), processed by the Gaia Data Processing and Analysis Consor-

tium (DPAC, http://www.cosmos.esa.int/web/gaia/dpac/consortium). Funding for the DPAC has been provided by national institutions, in particular the institutions participating in the Gaia Multilateral Agreement. This publication makes use of data products from the Wide-field Infrared Survey Explorer, which is a joint project of the University of California, Los Angeles, and the Jet Propulsion Laboratory/California Institute of Technology, funded by the National Aeronautics and Space Administration.

Facilities: Gaia,WISE

REFERENCES

Astraatmadja, T. L., & Bailer-Jones, C. A. L. 2016, ArXiv e-prints, arXiv:1609.07369
Bailer-Jones, C. A. L. 2015, PASP, 127, 994
Benedict, G. F., McArthur, B. E., Feast, M. W., et al. 2007, AJ, 133, 1810
—. 2011, AJ, 142, 187
Casertano, S., Riess, A. G., Bucciarelli, B., & Lattanzi, M. G. 2016, ArXiv e-prints, arXiv:1609.05175
Catelan, M., Pritzl, B. J., & Smith, H. A. 2004, ApJS, 154, 633
Cramér, H. 1999, Mathematical Methods of Statistics, Princeton landmarks in mathematics and physics (Princeton University Press)
Dambis, A. K., Rastorguev, A. S., & Zabolotskikh, M. V. 2014, MNRAS, 439, 3765
De Ridder, J., Molenberghs, G., Eyer, L., & Aerts, C. 2016, A&A, 595, L3
Feast, M. W., & Catchpole, R. M. 1997, MNRAS, 286, L1
Fernley, J., Barnes, T. G., Skillen, I., et al. 1998, A&A, 330, 515
Foreman-Mackey, D., Hogg, D. W., Lang, D., & Goodman, J. 2013, PASP, 125, 306
Gaia Collaboration, Brown, A. G. A., Vallenari, A., et al. 2016, ArXiv e-prints, arXiv:1609.04172
Goodman, J., & Weare, J. 2010, Commun. Appl. Math. Comput. Sci., 5, 65
Gould, A., Kollmeier, J. A., & Sesar, B. 2016, ArXiv e-prints, arXiv:1609.06315
Jao, W.-C., Henry, T. J., Riedel, A. R., et al. 2016, ArXiv e-prints, arXiv:1611.00656
Jaynes, E. T. 1968, IEEE Transactions on Systems Science and Cybernetics, 4, 227
Klein, C. R., Richards, J. W., Butler, N. R., & Bloom, J. S. 2011, ApJ, 738, 185
—. 2014, MNRAS, 440, L96
Koller, D., & Friedman, N. 2009, Probabilistic Graphical Models: Principles and Techniques - Adaptive Computation and Machine Learning (The MIT Press)
Leavitt, H. S. 1908, Annals of Harvard College Observatory, 60, 87
Leavitt, H. S., & Pickering, E. C. 1912, Harvard College Observatory Circular, 173, 1
Lindegren, L., Lammers, U., Bastian, U., et al. 2016, ArXiv e-prints, arXiv:1609.04303
Madore, B. F., Hoffman, D., Freedman, W. L., et al. 2013, ApJ, 776, 135
Marconi, M., Coppola, G., Bono, G., et al. 2015, ApJ, 808, 50
Michalik, D., Lindegren, L., & Hobbs, D. 2015, A&A, 574, A115
Nemec, J. M., Cohen, J. G., Ripepi, V., et al. 2013, ApJ, 773, 181
Schlafly, E. F., Meisner, A. M., Stutz, A. M., et al. 2016, ApJ, 821, 78
Schlegel, D. J., Finkbeiner, D. P., & Davis, M. 1998, ApJ, 500, 525
Sollima, A., Cacciari, C., & Valenti, E. 2006, MNRAS, 372, 1675
Stassun, K. G., & Torres, G. 2016, ArXiv e-prints, arXiv:1609.05390
van Leeuwen, F., Feast, M. W., Whitelock, P. A., & Yudin, B. 1997, MNRAS, 287, 955
Wright, E. L., Eisenhardt, P. R. M., Mainzer, A. K., et al. 2010, AJ, 140, 1868

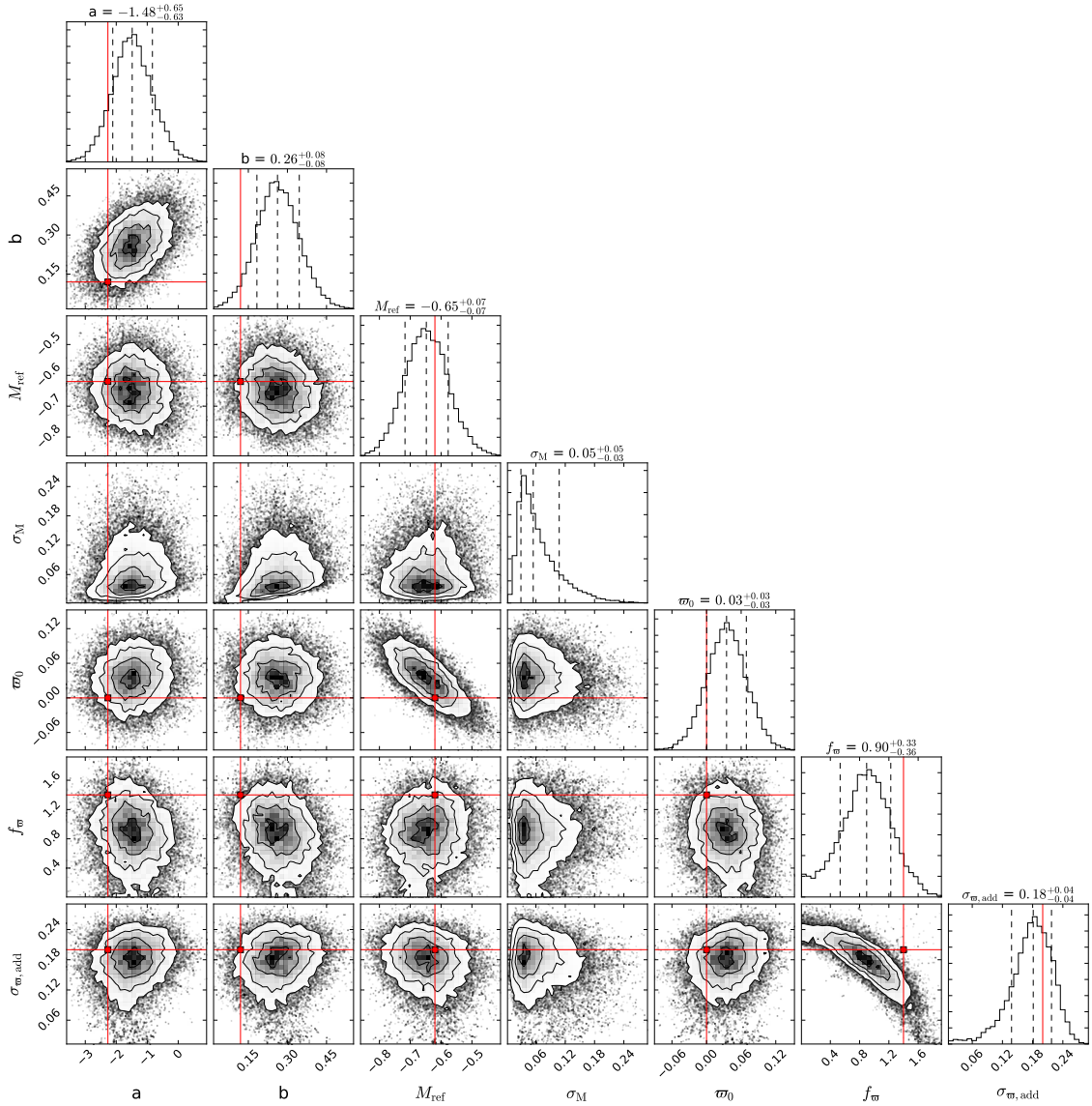

Figure 2. Posterior distributions of parameters in $\theta_{\rm PLZ}$ and θ_ϖ sets, for the parameters constrained using W2 band data. The histograms show the marginalized posterior distributions for each parameter, with the dashed lines indicating the 16th percentile, the median, and the 84th percentile. The contour plots show the two-dimensional posterior distributions for parameter pairs, with the contours indicating 0.5σ, 1σ, 1.5σ, and 2σ levels. Uncorrelated pairs have roundish contours, while correlated parameters like f_ϖ vs. $\sigma_{\varpi,\rm add}$ have elongated distributions. For comparison, the red squares and lines show the best-fit values of a, b, and $M_{\rm ref}$ measured by Dambis et al. (2014), the $\varpi_0 = 0$ mas line, and the f_ϖ and $\sigma_{\varpi,\rm add}$ values adopted by Lindegren et al. (2016).